Magnetic impurity in a Weyl semimetal

Jin-Hua Sun,[1,2] Dong-Hui Xu,[3] Fu-Chun Zhang,[1,2] and Yi Zhou[1,2]
[1]*Department of Physics, Zhejiang University, Hangzhou 310027, China*
[2]*Collaborative Innovation Center of Advanced Microstructures, Nanjing 210093, China*
[3]*Department of Physics, Hong Kong University of Science and Technology, Clearwater Bay, Kowloon, Hong Kong, China*
(Received 17 September 2015; published 12 November 2015)

We utilize the variational method to study the Kondo screening of a spin-1/2 magnetic impurity in a three-dimensional (3D) Weyl semimetal with two Weyl nodes along the k_z axis. The model reduces to a 3D Dirac semimetal when the separation of the two Weyl nodes vanishes. When the chemical potential lies at the nodal point, $\mu = 0$, the impurity spin is screened only if the coupling between the impurity and the conduction electron exceeds a critical value. For finite but small μ, the impurity spin is weakly bound due to the low density of states, which is proportional to μ^2, contrary to that in a 2D Dirac metal such as graphene and 2D helical metal, where the density of states is proportional to $|\mu|$. The spin-spin correlation function $J_{uv}(\mathbf{r})$ between the spin v component of the magnetic impurity at the origin and the spin u component of a conduction electron at spatial point $\mathbf{r}$ is found to be strongly anisotropic due to the spin-orbit coupling, and it decays in the power law. The main difference of the Kondo screening in 3D Weyl semimetals and in Dirac semimetals is in the spin x (y) component of the correlation function in the spatial direction of the z axis.

DOI: 10.1103/PhysRevB.92.195124 PACS number(s): 71.20.Be, 75.20.Hr, 03.65.Vf, 71.27.+a

I. INTRODUCTION

Two-dimensional (2D) Dirac fermions have been proposed and observed in graphene [1–3] and in surface states of 3D topological insulators (TIs) [4–6]. 3D Dirac semimetal represents a new state of quantum matter, which can host 3D Dirac fermions in the bulk [7]. The stable 3D Dirac semimetals have been realized experimentally in Na_3Bi compounds [8] and Cd_3As_2 crystals [9,10], where the Dirac points are stabilized by crystalline symmetry and the Dirac nodes are degenerate. If the inversion ($\mathcal{P}$) or time-reversal ($\mathcal{T}$) symmetry is broken, each Dirac node splits into two Weyl nodes resulting in Weyl semimetals [11–13]. Weyl semimetals show interesting physics such as Fermi arc surface states and chiral anomaly. Recently, Weyl semimetals have attracted much attention because a new TaAs family of Weyl semimetals has been predicted in theories [14,15] and subsequently observed in experiments [16–23].

A single magnetic impurity [24] in a conventional metal is well described by the Anderson impurity model. This model or the Kondo problem [25] has been widely studied by using various methods [26–34]. The impurity spin-1/2 is fully screened, and the correlation between the impurity spin and a conduction electron of distance r is of a power-law decay $1/r^d$ if $r < \xi_K$ and $1/r^{d+1}$ if $r > \xi_K$, with ξ_K the Kondo coherence length and d the dimensionality of the host metal [35–37]. Graphene has a peculiar electron structure, where the density of states (DOS) vanishes at a charge neutral point or at half-filling. The property of a magnetic impurity in half-filled graphene falls into the category of a pseudogap Kondo problem [38–40], which has been studied consistently using various methods including the numerical renormalization group (NRG). In single-layer graphene, the full screening of a magnetic impurity requires a finite strength of the hybridization between the impurity and Dirac electrons, and the spin-spin correlation between the impurity and conduction electron decays with $1/r^3$ power law for large r [41]. Recently, the Kondo effect in 3D Dirac and Weyl systems was studied using the NRG method, and it was found that the magnetic impurity shows a diverse range of Kondo physics, depending on the DOS of the host system and the symmetries broken by perturbations [42]. The spin-spin correlation in the spin-orbit coupled systems may be interesting since the coupling between the spin and the momentum results in anisotropy in both the spin and spatial spaces.

The purpose of this paper is to investigate the properties of spin-spin correlation in Dirac and Weyl semimetals. We study the binding energy and the various components of spin-spin correlation, and we illustrate the similarity or differences between the Dirac and Weyl semimetals. The variational method we apply has been used to study the ground state of the Kondo problem in conventional metals [33,43], antiferromagnets [44], and 2D helical metals [45].

The paper is organized as follows. We present the model and dispersion relation in Sec. II. In Sec. III, we apply the variational method to study the binding energy. In Sec. IV, we investigate the spin-spin correlation between the magnetic impurity and the conduction electrons in Dirac or Weyl semimetals, and we compare the results in these two systems. Finally, the discussions and conclusions are given in Sec. V.

II. ANDERSON MODEL HAMILTONIAN

We utilize the Anderson impurity model to study the Kondo screening of a spin-1/2 magnetic impurity in a 3D Dirac or Weyl semimetal. The model Hamiltonian contains three parts: the kinetic energy H_0 of the Dirac or Weyl semimetal, the impurity Hamiltonian H_d, and the hybridization between the impurity and the Dirac or Weyl semimetal H_V. The Hamiltonian reads

$$H = H_0 + H_d + H_V. \tag{1}$$

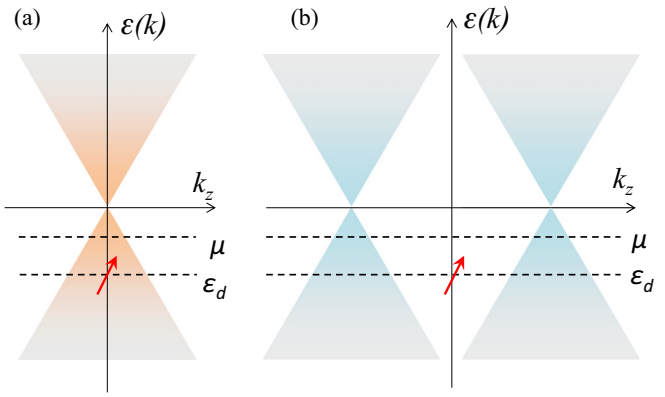

FIG. 1. (Color online) Schematics of the dispersion relation of (a) Dirac semimetals and (b) Weyl semimetals along the k_z axis. The Dirac cones are located at $k_z = 0$ in the Dirac semimetals, and the Weyl nodes are located at $k_z = \pm b/(2\lambda)$ in the Weyl semimetals. μ is the chemical potential and ε_d is the energy level of the Anderson impurity.

Here the kinetic energy part is given by

$$H_0 = \sum_{\mathbf{k}} \Psi_{\mathbf{k}}^{\dagger}[2\lambda\sigma_z(\mathbf{S}\times\mathbf{k})\cdot\hat{z} + 2\lambda_z\sigma_y k_z + \sigma_x M_{\mathbf{k}} + bS_z - \mu]\Psi_{\mathbf{k}},$$
$$= \sum_{\mathbf{k}} \Psi_{\mathbf{k}}^{\dagger} \begin{pmatrix} b-\mu & 2i\lambda k_- & -2i\lambda k_z & 0 \\ -2i\lambda k_+ & -b-\mu & 0 & -2i\lambda k_z \\ 2i\lambda k_z & 0 & b-\mu & -2i\lambda k_- \\ 0 & 2i\lambda k_z & 2i\lambda k_+ & -b-\mu \end{pmatrix} \Psi_{\mathbf{k}}, \tag{2}$$

where $\mathbf{k} = (k_x, k_y, k_z)$ and $k_\pm = k_x \pm ik_y$. σ, $\mathbf{S}$ are Pauli matrices in orbital and spin spaces, respectively. The basis vectors of the bulk states are chosen as $\Psi_{\mathbf{k}} = (a_{\mathbf{k}\uparrow}, a_{\mathbf{k}\downarrow}, b_{\mathbf{k}\uparrow}, b_{\mathbf{k}\downarrow})^T$, where a and b are orbital indices. $M_{\mathbf{k}} = M - tk^2$, with M the Dirac mass. For $\lambda_z > 0$ and $M < 0$, H_0 describes a strong topological insulator with Z_2 index (1; 000). Here we shall consider the case with $M = 0$ while the bulk gap closes at $\mathbf{k} = \mathbf{0}$ and a transition between a topologically nontrivial phase and a trivial phase occurs. For simplicity, we shall assume that $\lambda_z = \lambda$ eliminates the extra anisotropy, and we set $M_{\mathbf{k}} = 0$ since the nonzero $M_{\mathbf{k}}$ merely modifies the high-energy dispersion, which has a minor influence on our study. At $b = 0$, the H_0 describes the Dirac semimetal. At $b \neq 0$, it describes a Weyl semimetal with broken time-reversal ($\mathcal{T}$) symmetry [6,13,46]. In a Dirac semimetal, the Dirac points are doubly degenerate [see Fig. 1(a)], while in a Weyl semimetal each Dirac point splits into two Weyl nodes due to the broken $\mathcal{T}$ or parity symmetry. We note that the Weyl semimetal studied in the present paper corresponds to the $\mathcal{T}$-broken case. For $b > 0$, the Weyl nodes are located at the points $(0,0,\pm b/2\lambda)$ on the k_z axis as shown in Fig. 1(b).

The local magnetic impurity Hamiltonian can be written as

$$H_d = (\varepsilon_d - \mu)(d_\uparrow^{\dagger} d_\uparrow + d_\downarrow^{\dagger} d_\downarrow) + U n_{d\uparrow} n_{d\downarrow}. \tag{3}$$

$d_{\uparrow(\downarrow)}^{\dagger}$ and $d_{\uparrow(\downarrow)}$ are the creation and annihilation operators of the spin-up (spin-down) state on the impurity site, and ε_d and U are the impurity energy level and on-site Coulomb repulsion, respectively.

Finally, the hybridization between the magnetic impurity and the host material is described by

$$H_V = \sum_{\mathbf{k}} d_{\mathbf{k}}^{\dagger} \hat{V} \Psi_{\mathbf{k}}. \tag{4}$$

$d_{\mathbf{k}} = (d_{\mathbf{k}\uparrow}, d_{\mathbf{k}\downarrow})^T$, where $d_{\mathbf{k}s}$ ($d_{\mathbf{k}s}^{\dagger}$) is the impurity annihilation (creation) operators in momentum space. $\hat{V}$ is the hybridization strength, and we assume the magnetic impurity is equally coupled to the four bands in the semimetal,

$$\hat{V} = \begin{pmatrix} V_k & 0 & V_k & 0 \\ 0 & V_k & 0 & V_k \end{pmatrix}. \tag{5}$$

The single-particle eigenenergy, $\varepsilon_j(\mathbf{k})$, with $j = 1,2,3,4$, can be obtained by diagonalizing the noninteracting Hamiltonian H_0, and it is given by

$$\begin{aligned} \varepsilon_1(\mathbf{k}) &= -\sqrt{4\lambda^2(k_x^2 + k_y^2) + (b - 2\lambda k_z)^2} - \mu, \\ \varepsilon_2(\mathbf{k}) &= -\sqrt{4\lambda^2(k_x^2 + k_y^2) + (b + 2\lambda k_z)^2} - \mu, \\ \varepsilon_3(\mathbf{k}) &= \sqrt{4\lambda^2(k_x^2 + k_y^2) + (b - 2\lambda k_z)^2} - \mu, \\ \varepsilon_4(\mathbf{k}) &= \sqrt{4\lambda^2(k_x^2 + k_y^2) + (b + 2\lambda k_z)^2} - \mu, \end{aligned} \tag{6}$$

where $b = 0$ and $b \neq 0$ correspond to the Dirac and Weyl semimetals, respectively. The corresponding eigenstates are given by

$$\begin{aligned} \gamma_{\mathbf{k}1} &= \frac{1}{\sqrt{C_1}}\{\phi_{1\mathbf{k}} a_{\mathbf{k}\uparrow} + 2i\lambda k_- a_{\mathbf{k}\downarrow} + i\phi_{1\mathbf{k}} b_{\mathbf{k}\uparrow} + 2\lambda k_- b_{\mathbf{k}\downarrow}\}, \\ \gamma_{\mathbf{k}2} &= \frac{1}{\sqrt{C_2}}\{-\phi_{2\mathbf{k}} a_{\mathbf{k}\uparrow} - 2i\lambda k_- a_{\mathbf{k}\downarrow} + i\phi_{2\mathbf{k}} b_{\mathbf{k}\uparrow} + 2\lambda k_- b_{\mathbf{k}\downarrow}\}, \\ \gamma_{\mathbf{k}3} &= \frac{1}{\sqrt{C_3}}\{\phi_{3\mathbf{k}} a_{\mathbf{k}\uparrow} + 2i\lambda k_- a_{\mathbf{k}\downarrow} + i\phi_{3\mathbf{k}} b_{\mathbf{k}\uparrow} + 2\lambda k_- b_{\mathbf{k}\downarrow}\}, \\ \gamma_{\mathbf{k}4} &= \frac{1}{\sqrt{C_4}}\{-\phi_{4\mathbf{k}} a_{\mathbf{k}\uparrow} - 2i\lambda k_- a_{\mathbf{k}\downarrow} + i\phi_{4\mathbf{k}} b_{\mathbf{k}\uparrow} + 2\lambda k_- b_{\mathbf{k}\downarrow}\}, \end{aligned} \tag{7}$$

where C_j are the normalization factors. The parameters $\phi_{l\mathbf{k}}$ ($l = 1,2,3,4$) are given by

$$\begin{aligned} \phi_{1\mathbf{k}} &= (b - 2\lambda k_z) - m_{\mathbf{k}}, \quad \phi_{2\mathbf{k}} = (b + 2\lambda k_z) - n_{\mathbf{k}}, \\ \phi_{3\mathbf{k}} &= (b - 2\lambda k_z) + m_{\mathbf{k}}, \quad \phi_{4\mathbf{k}} = (b + 2\lambda k_z) + n_{\mathbf{k}}, \end{aligned} \tag{8}$$

where $m_{\mathbf{k}}(n_{\mathbf{k}}) = \sqrt{4\lambda^2(k_x^2 + k_y^2) + (b \mp 2\lambda k_z)}$. We can rewrite the total Hamiltonian H in the diagonal basis as

$$H = \sum_{\mathbf{k}j}[\varepsilon_j(\mathbf{k}) - \mu]\gamma_{\mathbf{k}j}^{\dagger}\gamma_{\mathbf{k}j} + \sum_{\mathbf{k}j} V_{\mathbf{k}}(\gamma_{\mathbf{k}j}^{\dagger} d_{\mathbf{k}j} + \text{H.c.}) + (\varepsilon_d - \mu)\sum_{\sigma} d_\sigma^{\dagger} d_\sigma + U\, d_\uparrow^{\dagger} d_\uparrow d_\downarrow^{\dagger} d_\downarrow, \tag{9}$$

where the impurity operators $d_{\mathbf{k}j}$ are given by

$$\begin{aligned} d_{\mathbf{k}1} &= \frac{(1+i)\phi_{1\mathbf{k}}}{\sqrt{C_1}}d_\uparrow + \frac{(1+i)2\lambda k_-}{\sqrt{C_1}}d_\downarrow, \\ d_{\mathbf{k}2} &= \frac{-(1-i)\phi_{2\mathbf{k}}}{\sqrt{C_2}}d_\uparrow + \frac{(1-i)2\lambda k_-}{\sqrt{C_2}}d_\downarrow, \\ d_{\mathbf{k}3} &= \frac{(1+i)\phi_{3\mathbf{k}}}{\sqrt{C_3}}d_\uparrow + \frac{(1+i)2\lambda k_-}{\sqrt{C_3}}d_\downarrow, \\ d_{\mathbf{k}4} &= \frac{-(1-i)\phi_{4\mathbf{k}}}{\sqrt{C_4}}d_\uparrow + \frac{(1-i)2\lambda k_-}{\sqrt{C_4}}d_\downarrow. \end{aligned} \tag{10}$$

III. THE BINDING ENERGY

We start from the simplest limit in which the magnetic impurity and the host material are decoupled from each other, namely $H_V = 0$. The ground-state wave function of H_0 can be written as

$$|\Psi\rangle_0 = \prod_{\mathbf{k}j;\varepsilon_j(\mathbf{k})<\mu} {\gamma_{\mathbf{k}j}}^\dagger |0\rangle, \tag{11}$$

where the product runs over all the states inside the Fermi surface. If $\varepsilon_d < \mu < \varepsilon_d + U$, the impurity is singly occupied with a local moment, and the impurity energy is $\varepsilon_d - \mu$. The total energy of the system is given by the sum of the energies of the host material and of the magnetic impurity,

$$E_0 = \varepsilon_d - \mu + \sum_{\mathbf{k}j;\varepsilon_j(\mathbf{k})<\mu} \varepsilon_j(\mathbf{k}). \tag{12}$$

In the above equations, the index $j = 1,2,3,4$ denotes the four bands in the Dirac or Weyl semimetal.

Now we study the effect of H_V, which describes the hybridization between the magnetic impurity and the host Weyl semimetal by using a variational method. We shall assume the large-U limit. In this case, we may neglect the doubly occupied impurity states in our trial wave function for the ground state, which is given by

$$|\Psi\rangle = \left(c_0 + \sum_{\mathbf{k}j} c_{\mathbf{k}j} d_{\mathbf{k}j}^\dagger \gamma_{\mathbf{k}j}\right)|0\rangle. \tag{13}$$

c_0 and $c_{\mathbf{k}j}$ are variational parameters to be determined by optimizing the ground-state energy. The energy of the Hamiltonian H in the trial state $|\Psi\rangle$ is given by

$$E = \frac{\sum_{\mathbf{k}j}\left\{[E_0 - \varepsilon_j(\mathbf{k}) + \mu]c_{kj}^2 + 2V_{\mathbf{k}}c_0 c_{\mathbf{k}j} + [\varepsilon_j(\mathbf{k}) - \mu]c_0^2\right\}}{c_0^2 + \sum_{\mathbf{k}j} c_{\mathbf{k}j}^2}. \tag{14}$$

The variational principle requires

$$\partial E/\partial c_0 = \partial E/\partial c_{\mathbf{k}j} = 0, \tag{15}$$

from which we obtain the following two equations:

$$\begin{aligned} Ec_0 &= \sum_{\mathbf{k}j}\{V_{\mathbf{k}}c_{\mathbf{k}j} + [\varepsilon_j(\mathbf{k}) - \mu]c_0\}, \\ Ec_{\mathbf{k}j} &= [E_0 - \varepsilon_j(\mathbf{k}) + \mu]c_{\mathbf{k}j} + V_{\mathbf{k}}c_0, \end{aligned} \tag{16}$$

which lead to

$$\begin{aligned} \left(E - \sum_{\mathbf{k}j}[\varepsilon_j(\mathbf{k}) - \mu]\right)c_0 &= \sum_{\mathbf{k}j} V_{\mathbf{k}}c_{\mathbf{k}j}, \\ \{E - E_0 + [\varepsilon_j(\mathbf{k}) - \mu]\}c_{\mathbf{k}j} &= V_{\mathbf{k}}c_0. \end{aligned} \tag{17}$$

We define the binding energy as $\Delta_b = E_0 - E$. If $\Delta_b > 0$, then the hybridized state has lower energy than the bare state, so that the hybridized state is more stable. From Eq. (17) we obtain

$$c_{\mathbf{k}j} = \frac{V_{\mathbf{k}}c_0}{[\varepsilon_j(\mathbf{k}) - \mu] - \Delta_b} \tag{18}$$

and

$$[E - E_0 + (\varepsilon_d - \mu)]c_0 = \sum_{\mathbf{k}j} V_{\mathbf{k}}c_{\mathbf{k}j}. \tag{19}$$

We then obtain the self-consistent equation,

$$(\varepsilon_d - \mu) - \Delta_b = \sum_{\mathbf{k}j} \frac{V_{\mathbf{k}}^2}{[\varepsilon_j(\mathbf{k}) - \mu] - \Delta_b}. \tag{20}$$

By solving Eq. (20) numerically, we obtain the binding energy Δ_b. From Eq. (18) we can calculate $c_{\mathbf{k}j}$ for given $\mathbf{k}$ and j. In the calculations, we introduce an energy cutoff Λ, and hence the truncation of momentum $k_c = \Lambda/(2\lambda)$. The summation over momentum in Eq. (20) is then replaced by an integration $\frac{1}{N}\sum_{\mathbf{k}} \to \frac{6\pi^2}{k_c^3}\int \frac{\mathbf{d}^3k}{(2\pi)^3}$.

One can see that the binding energy is independent of the host system to be the Dirac or Weyl semimetal. Although the Weyl nodes are located at $k_z = \pm b/2\lambda$ in the Weyl semimetal, the dispersion relation around each Weyl node is exactly the same as those around the Dirac cones, thus the summation over k on the right-hand side of Eq. (20) shall also remain the same. We define an effective hybridization $\Gamma = \frac{3V_k^2}{\Lambda^2}$. From Eq. (20) we obtain

$$\begin{aligned} &(\varepsilon_d - \mu) - \Delta_b + \Gamma\left[\frac{(\Lambda^2 - \mu^2)}{\Lambda} - 2\frac{(\Lambda - |\mu|)(\mu + \Delta_b)}{\Lambda}\right] \\ &\quad = -2\Gamma\frac{(\mu + \Delta_b)^2}{\Lambda}\ln\frac{\Lambda + \mu + \Delta_b}{\Delta_b}. \end{aligned} \tag{21}$$

Then in the limit of small Γ and $\Gamma\Lambda < \mu - \varepsilon_d + 2\Gamma\mu$, we have

$$\Delta_b \approx \Lambda \exp\left\{-\frac{\mu - \varepsilon_d - \Gamma\Lambda + 2\Gamma\mu}{2\Gamma\mu^2/\Lambda}\right\} \ (\mu \neq 0). \tag{22}$$

If $\mu \neq 0$, the hybridization shall always lead to a finite binding energy $\Delta_b > 0$. However, if $\mu = 0$, Eq. (21) gives rise to

$$\varepsilon_d + \Gamma\Lambda = \Delta_b - \frac{2\Gamma}{\Lambda}\Delta_b^2 \ln\frac{\Lambda}{\Delta_b}. \tag{23}$$

In the limit of small Γ, we obtain $\Delta_b \approx \varepsilon_d + \Gamma\Lambda$. The density of states in the Dirac or Weyl semimetal vanishes, hence the binding energy Δ_b has a positive solution only when the effective hybridization Γ is above a critical value, $\Gamma > \frac{|\varepsilon_d|}{\Lambda}$. This is similar to the case of graphene [47,48] and other 2D helical metals [45]. In the context of Kondo physics, it is the so-called pseudogap Kondo problem [38–40].

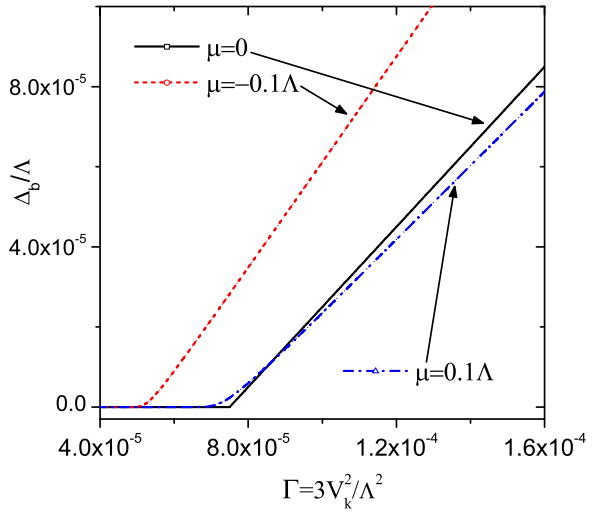

FIG. 2. (Color online) Calculated binding energy Δ_b of a magnetic impurity in Dirac or Weyl semimetal as a function of Γ for three values of chemical potential μ. Λ is the energy cutoff, and $\Gamma = 3V_k^2/\Lambda^2$ is the effective hybridization. At $\mu = 0$, there is a threshold $\Gamma > \Gamma_c = |\epsilon_d|/\Lambda = 7.5 \times 10^{-5}$ for the bound state. For $\mu \neq 0$, Δ_b is finite, but it is too small to be seen in the figure for small Γ.

The self-consistent solution of the binding energy is plotted in Fig. 2 as a function of the effective hybridization Γ. We fix the value of $\mu - \epsilon_d = 7.5 \times 10^{-5}\Lambda$, and the chemical potential is chosen as $\mu = 0$ and $\mu = \pm 0.1\Lambda$. While $\mu = 0$ the system is at half-filling, and we can see that the binding energy Δ_b is nonzero only if the effective hybridization is greater than the critical value $\Gamma_c = |\epsilon_d|/\Lambda = 7.5 \times 10^{-5}$. While $\mu \neq 0$ the binding energy always has a positive value, which can also be seen from the analytical results shown in Eq. (22). The DOS $D(E) \propto E^2$ is much smaller than that in graphene near the charge neutral point, so that the screening effect and thus the binding energy are much smaller than those in the graphene case. The asymmetry between the $\mu = \pm 0.1\Lambda$ cases is due to the asymmetry of the impurity state between being empty and doubly occupied.

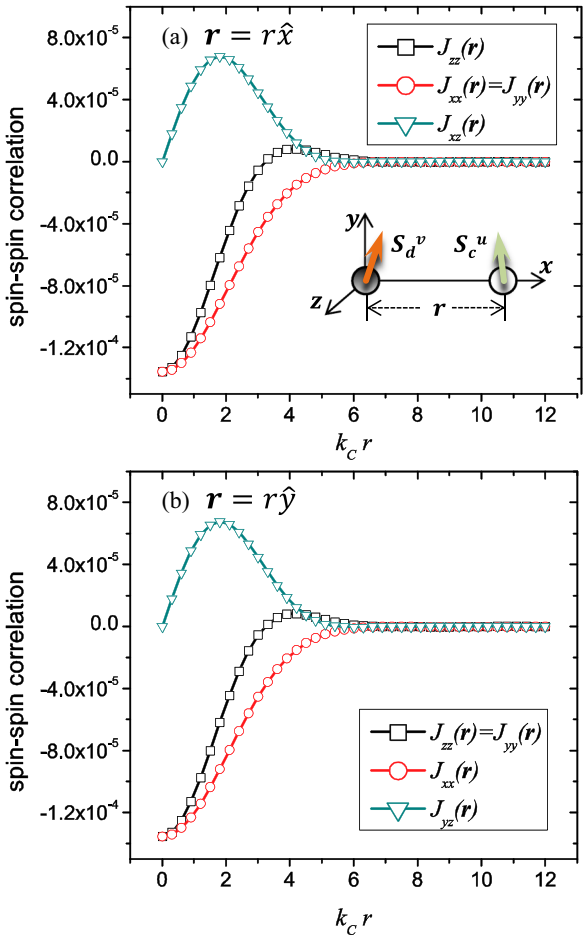

FIG. 3. (Color online) Spin-spin correlation between the magnetic impurity and the conduction electron along the x axis (a) and along the y axis (b). The results are the same for the Dirac or Weyl semimetal. The inset in (a) illustrates spin S_d^v of the magnetic impurity at the origin $r = 0$ and the conduction electron spin S_c^u at a distance r along the x axis. The parameters are $\mu = -0.01\Lambda$, $V_k = 0.05\Lambda$, and $\Delta = 0.05\Lambda$, and the energy cutoff Λ is large enough that the value of Λ will not affect the low-energy physics. All the other spin-spin correlations not shown here are zero.

IV. SPIN-SPIN CORRELATION BETWEEN MAGNETIC IMPURITY AND CONDUCTION ELECTRONS

Now we study the spin-spin correlation between the magnetic impurity $S_d = \frac{1}{2}d^\dagger\sigma d$ and the conduction electron spin $S_c = \frac{1}{2}c^\dagger\sigma c$ in the Dirac or Weyl semimetal. The impurity-spin–conduction-electron-spin correlation function is evaluated for $\mu \neq 0$ while the binding energy Δ_b always has a positive value, i.e., there exists Kondo screening. We assume that the impurity is located at the origin $\mathbf{r} = \mathbf{0}$, and we only consider the simplest case in which the spin-spin correlation function is evaluated along the three axes: the x, y, and z axes. The spin-spin correlation function between the magnetic impurity and the conduction electron is given by

$$J_{uv}(\mathbf{r}) = \langle S_c^u(\mathbf{r}) S_d^v(0) \rangle, \tag{24}$$

where $u, v = x, y, z$ and $\langle \cdots \rangle$ denotes the ground-state average. We start with simple symmetry analysis. As we have mentioned, the Dirac semimetals we study in this paper preserve both $\mathcal{P}$ and $\mathcal{T}$ symmetries, while in Weyl semimetals the $\mathcal{T}$ symmetry is broken due to the displacement of the Dirac cones along the k_z axis. Both of the systems have rotational symmetry along the z axis, so we have $J_{uv}(\mathbf{r}) = J_{u'v'}(\mathbf{r}')$ if $u' = \mathcal{R}_z(\beta)u$, $v' = \mathcal{R}_z(\beta)v$, $r' = \mathcal{R}_z(\beta)r$, where $\mathcal{R}_z(\beta)$ is a rotational operator along the z axis. Actually, one can demonstrate that both systems are unchanged under a combined mirror reflection and time-reversal transformation. We may denote the mirror reflection with respect to the y-z plane as $\mathcal{M}^{yz}$. Then we have $\mathcal{TM}^{yz}(x, y, z) = (-x, y, z)$, $\mathcal{TM}^{yz}(k_x, k_y, k_z) = (k_x, -k_y, -k_z)$, and $\mathcal{TM}^{yz}(S_x, S_y, S_z) = (-S_x, S_y, S_z)$. Thus if $\mathbf{r}$ is on the x, y, or z axis, we can easily find that only $J_{yz}(r\hat{y}) = -J_{zy}(r\hat{y})$ and $J_{xz}(r\hat{x}) = -J_{zx}(r\hat{x})$ are nonzero among the off-diagonal terms. We should emphasize that due to the absence of the spin SU(2) symmetry, the

off-diagonal terms can generally be nonzero in coordinate space, but we may only concentrate on the three spatial axes in this present paper.

We can define functions below and use them to simplify the spin-spin correlation function in coordinate space,

$$\begin{aligned} I_j(\mathbf{r}) &= \sum_k e^{-i\mathbf{k}\cdot\mathbf{r}}\frac{\phi_{kj}}{C_j}c_{kj}, \quad J_j(\mathbf{r}) = \sum_k e^{-i\mathbf{k}\cdot\mathbf{r}}\frac{\phi_{kj}}{C_j}2\lambda(-ik_+)c_{kj}, \\ T_j(\mathbf{r}) &= \sum_k e^{-i\mathbf{k}\cdot\mathbf{r}}\frac{\phi_{kj}}{C_j}2\lambda(ik_-)c_{kj}, \quad Y_j(\mathbf{r}) = \sum_k e^{-i\mathbf{k}\cdot\mathbf{r}}c_{kj}, \\ Q_j(\mathbf{r}) &= \sum_k e^{-i\mathbf{k}\cdot\mathbf{r}}\frac{4\lambda^2\left(k_x^2+k_y^2\right)}{C_j}c_{kj} = \frac{1}{2}Y_j - I_j. \end{aligned} \tag{25}$$

Here again $j = 1,2,3,4$ are used to denote the four bands in the Dirac or Weyl semimetals. Then the diagonal terms and the nonzero off-diagonal terms of the spin-spin correlation function along the three axes are given by

$$\begin{aligned} J_{zz}(\mathbf{r}) &= -\{[|I_1+I_3|^2+|I_2+I_4|^2+|Q_1+Q_3|^2+|J_2+J_4|^2-|J_1+J_3|^2-|J_2+J_4|^2-|T_1+T_3|^2-|T_2+T_4|^2]\}, \\ J_{xx}(\mathbf{r}) &= -\{2[(J_1+J_3)(T_2^*+T_4^*)+(J_2+J_4)(T_1^*+T_3^*)+(I_1+I_3)(Q_2^*+Q_4^*)+(I_2+I_4)(Q_1^*+Q_3^*)]\}, \\ J_{yy}(\mathbf{r}) &= -\{2[-(J_1+J_3)(T_2^*-T_4^*)+(J_2+J_4)(T_1^*+T_3^*)+(I_1+I_3)(Q_2^*+Q_4^*)+(I_2+I_4)(Q_1^*+Q_3^*)]\}, \\ J_{xz}(\mathbf{r}) &= -2\,\mathrm{Re}\{[I_1+I_3+i(I_2+I_4)][T_1^*+T_3^*-i(T_2^*+T_4^*)]-[J_1+J_3-i(J_2+J_4)][Q_1^*+Q_3^*+i(Q_2^*+Q_4^*)]\}, \\ J_{yz}(\mathbf{r}) &= -2\,\mathrm{Im}\{[I_1+I_3+i(I_2+I_4)][T_1^*+T_3^*-i(T_2^*+T_4^*)]-[J_1+J_3-i(J_2+J_4)][Q_1^*+Q_3^*+i(Q_2^*+Q_4^*)]\}. \end{aligned} \tag{26}$$

If we consider the simplest case when $\mu < 0$ and $b = 0$, then we have $m = 2\lambda k$ and $\phi_{1k} = -2\lambda(k+k_z) = -2\lambda k(1+\cos\theta)$, and then the correlation reads

$$J_{zz} \propto |I_1|^2 + |I_2|^2 + |Q_1|^2 + |Q_2|^2. \tag{27}$$

We take the first term for example,

$$\begin{aligned} I_1 &= \sum_k e^{-i\mathbf{k}\cdot\mathbf{r}}\frac{\phi_{1k}^2}{C_1}c_{k1} = \sum_k e^{-i\mathbf{k}\cdot\mathbf{r}}\frac{\phi_{1k}^2}{-4m\phi_{1k}}c_{k1} \\ &= \sum_k e^{-i\mathbf{k}\cdot\mathbf{r}}\frac{\phi_{1k}}{-4m_k}c_{k1} = \frac{1}{4}\sum_k e^{-i\mathbf{k}\cdot\mathbf{r}}(1+\cos\theta)c_{k1}. \end{aligned} \tag{28}$$

After a straightforward integration, we obtain

$$\begin{aligned} I_1 \propto{}& \frac{i}{r}\left(e^{-i\frac{\Lambda}{2\lambda}r} - e^{-i\frac{|\mu|}{2\lambda}r}\right) \\ &- \frac{\mu+\Delta_b}{2\lambda}e^{i\frac{(\mu+\Delta_b)r}{2\lambda}}\int_{r\Delta_b/2\lambda}^{r\Lambda/2\lambda}\frac{e^{-iy}}{y}dy. \end{aligned} \tag{29}$$

By assuming $\mu + \Delta_b \ll \Lambda$, we can ignore the second term and obtain

$$I_1 = -\frac{3iV_k a_0}{4\Lambda}\frac{1}{(k_c r)^2}\left(e^{-i\frac{\Lambda}{2\lambda}r} - e^{-i\frac{|\mu|}{2\lambda}r}\right), \tag{30}$$

where a_0 is the number defined in Eq. (13), and Λ is the energy cutoff. We can easily find that $I_2 = I_1$, and Q_1 and Q_2 also decay with $1/(k_c r)^2$, which indicates that the spin-spin correlation $J_{zz}(r)$ follows a $1/(k_c r)^4$ decay at long distance. Using a similar analysis, we can see that while $b = 0$, all the other diagonal and off-diagonal components of the spin-spin correlation decay with $1/(k_c r)^4$ in real space. The results for the Weyl semimetal ($b \neq 0$) are more complicated, which will be discussed later.

In Fig. 3, we show the results of $J_{uv}(r)$ for r along the x and y axes. The values of $J_{uv}(r)$ along these two axes are independent of b, hence they are the same for the Dirac and Weyl semimetals. As shown in Fig. 3, the diagonal terms are all antiferromagnetic at short distance. In Fig. 3(a) for $\mathbf{r}$ along the x axis, we have $J_{xx}(r) = J_{yy}(r) \neq J_{zz}(r)$, and only two of the off-diagonal terms, $J_{xz}(r) = -J_{zx}(r)$, are nonzero. The inset in Fig. 3(a) shows the schematics of the displacement of the magnetic impurity and the conduction electrons. We assume the location of the impurity is at $r = 0$ and the conduction electron is on the x axis, and the displacement between them is r. S_d^v and S_c^u are used to denote the spins on the magnetic impurity and the conduction electron, respectively. Similarly, in Fig. 3(b) we have $J_{yy} = J_{zz} \neq J_{xx}$ and only one off-diagonal term J_{yz} is nonzero. The off-diagonal terms reflect the spin-orbit coupling in the Dirac and Weyl semimetals.

In Fig. 4, we show the spin-spin correlation with $\mathbf{r}$ along the z axis, which depends on b, hence it is different between the Dirac and Weyl semimetals. First, in the 3D Dirac system, the diagonal terms are all equivalent, $J_{xx} = J_{yy} = J_{zz}$. As the value of b increases, the Dirac cones split and Weyl nodes emerge. One can see that $J_{zz}(r)$ remains the same as b increases. We always have $J_{zz}(r)|_{b=0} = J_{zz}(r)|_{b>0} = J_{xx}(r)|_{b=0} = J_{yy}(r)|_{b=0}$ if r is along the z axis. We still have $J_{xx} = J_{yy}$ for $b > 0$, and we find that these two terms are modified in the coordinate space as b increases. If $\mu < 0$ and $\mathbf{r} = r\hat{z}$, then from Eq. (26) we obtain

$$J_{xx}(r\hat{z}) = -2\left(J_1T_2^* + J_2T_1^* + I_1Q_2^* + I_2Q_1^*\right), \tag{31}$$

where the indices 1 and 2 denote the lower bands whose Weyl nodes are located at $k_z = -b/2\lambda$ and $b/2\lambda$, respectively. J_1 corresponds to the contribution from the lower band whose Weyl node is at $k_z = -b/2\lambda$. If we perform a simple translation along the k_z axis and substitute k_z with $k_z' + b/2\lambda$, we obtain $J_1 = J_1^D e^{-i\frac{b}{2\lambda}r}$, where J_1^D is the result for Dirac semimetal. Similarly, we can see that $T_2^* = T_2^{D*}e^{-i\frac{b}{2\lambda}r}$, such

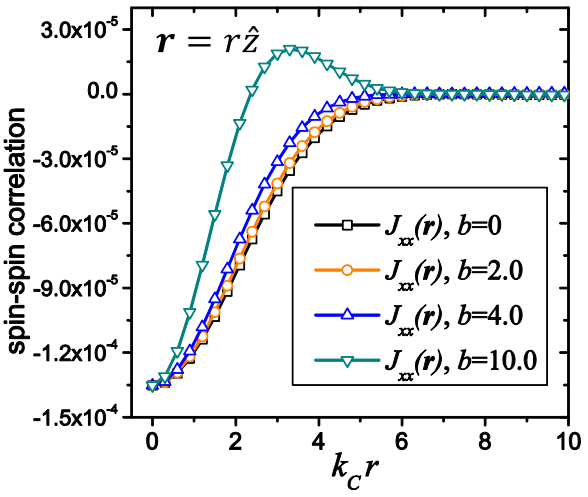

FIG. 4. (Color online) Spin-spin correlation between a magnetic impurity at the origin and a conduction electron at a distance r along the z axis for Dirac semimetal ($b = 0$) and Weyl semimetal of three values of b. The two Weyl nodes are at b/λ along the k_z axis. Correlation for spins along z, $J_{zz}(r)$, is independent of b and $J_{zz}(r)|_b = J_{xx}|_{b=0} = J_{yy}|_{b=0}$, while $J_{xx}(r)$ and $J_{yy}(r)$ are b-dependent. The parameters are $\mu = -0.01\Lambda$, $V_k = 0.05\Lambda$, and $\Delta = 0.05\Lambda$.

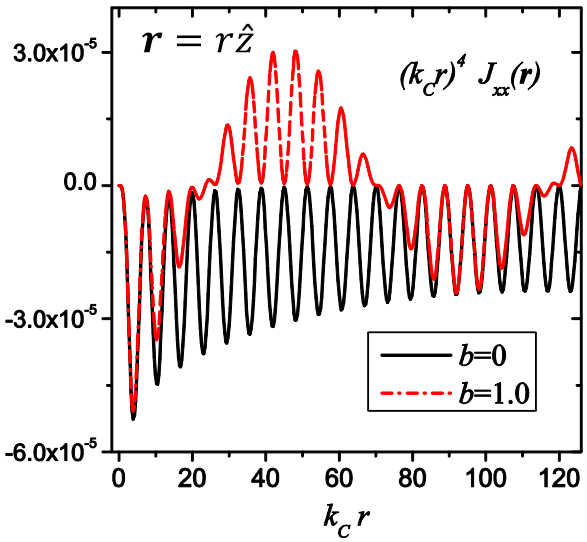

FIG. 5. (Color online) The product $(k_c r)^4 J_{xx}$ as a function of the dimensionless distance $k_c r$. Here the displacement $\mathbf{r}$ is along the z axis. We use $\mu = -0.01\Lambda$, $V_k = 0.05\Lambda$, and $\Delta = 0.05\Lambda$. The magnetic impurity is coupled to (a) Dirac semimetals ($b = 0$) and (b) Weyl semimetals ($b = 1$), respectively.

that $J_1 T_2^* = J_1^D T_2^{D*} e^{-i\frac{b}{\lambda}r}$ and $J_2 T_1^* = J_2^D T_1^{D*} e^{i\frac{b}{\lambda}r}$. Given that the two lower bands are degenerate at $b = 0$, we obtain

$$J_{xx}(r\hat{z}) = J_{xx}^D(r\hat{z})\cos(br/2\lambda), \tag{32}$$

where $J_{xx}^D(r\hat{z})$ is the x-x spin-spin correlation along the z axis in the Dirac semimetal, and $b/2\lambda$ is half of the separation of the two Weyl nodes along the k_z axis. One can easily find that the displacement of the Weyl nodes along the k_z axis will add an extra phase factor to each function defined in Eq. (25), and it will further induce complexity to the oscillation behavior of the spin-spin correlations along the z axis. One can use a similar approach to prove that for the y-y correlation it shall be $J_{yy}(r\hat{z}) = J_{yy}^D(r\hat{z})\cos(br/2\lambda)$. Generally in the short distance limit, as shown in Fig. 4, the spin-spin correlation decays faster as b increases.

Shown in Fig. 5 is the product $(k_c r)^4 J_{xx}(r)$ as a function of the dimensionless distance $k_c r$. We use $\mu = -0.01\Lambda$, $V_k = 0.05\Lambda$, and $\Delta = 0.05\Lambda$. We can see that both terms for $b = 0$ and 1.0 oscillate in coordinate space, and the decay rate is proportional to $(k_c r)^{-4}$. This decay rate is consistent with the general results in normal metals that the spin-spin correlation decays with r^{d+1} ($d = 3$) at far displacement. By carefully examining Eq. (26), we find that the effect of b is to add an extra phase factor to the spin-spin correlations, i.e., as the phase factor $\cos(br/2\lambda)$ added to the spin-spin correlation $J_{xx}^D(r\hat{z})$ given in Eq. (32). The results for different values of b generally have similar contributions, i.e., that the oscillation in the coordinate space is modified by b.

V. DISCUSSION AND CONCLUSION

In conclusion, we have studied spin-1/2 Anderson impurity in a Dirac or Weyl semimetal. We apply the variational method to study the problem at the large-U limit. Due to the spin-orbit coupling in these two systems, the spatial spin-spin correlations between the magnetic impurity and the conduction electron are highly anisotropic. The results of the binding energy are quite similar to those in graphene and 2D helical metals, and they are found to be the same for the Dirac and Weyl semimetal. Due to the vanishing DOS at half-filling, there exists a critical value of the effective hybridization strength. We may obtain a positive binding energy only if the hybridization is above the critical value. While the system is particle-hole asymmetric, the DOS at the Fermi surface becomes finite, such that the hybridization always leads to a positive binding energy. However, due to the fact that the DOS near the Weyl points is proportional to E^2, the screening effect of the conduction electrons is much weaker than that in graphene, in which $\mathrm{DOS}(E) \propto |E|$. Therefore, in the weak hybridization limit and at the chemical potential near the Dirac point, the impurity binding energy in the 3D Dirac or Weyl semimetal is much smaller than that in the corresponding graphene system or 2D helical metal.

The spin-spin correlations in both the Dirac and Weyl semimetal are highly asymmetric in coordinate space due to the spin-orbit coupling. Although the Kondo temperature of a Dirac or Weyl semimetal is mainly determined by the DOS and not affected by the spin-orbit coupling [49], the spin-spin correlation we study here shows rich features spatially. In general, the diagonal terms decay with r^{-4} for $\mu \neq 0$, which is in agreement with the results in normal 3D metals. The spin-spin correlations are independent of the Dirac or Weyl semimetal, except for the spatial separation between the impurity and conduction electron along the z axis. In that case, the momentum $b/2\lambda$ adds an extra phase factor to spin-spin correlation $J_{xx}(r)$ and $J_{yy}(r)$, so that the spin-spin correlation is modified according to b.

ACKNOWLEDGMENTS

This work is supported in part by the National Basic Research Program of China (2014CB921201/2014CB921203), NSFC (No. 11374256/11274269), and the Fundamental Research Funds for the Central Universities in China.

[1] K. Novoselov, A. Geim, S. Morozov, D. Jiang, Y. Zhang, S. Dubonos, I. Grigorieva, and A. Firsov, Science **306**, 666 (2004).
[2] A. H. Castro Neto, F. Guinea, N. M. R. Peres, K. S. Novoselov, and A. K. Geim, Rev. Mod. Phys. **81**, 109 (2009).
[3] V. N. Kotov, B. Uchoa, V. M. Pereira, F. Guinea, and A. H. Castro Neto, Rev. Mod. Phys. **84**, 1067 (2012).
[4] J. E. Moore, Nature (London) **464**, 194 (2010).
[5] M. Z. Hasan and C. L. Kane, Rev. Mod. Phys. **82**, 3045 (2010).
[6] X.-L. Qi and S.-C. Zhang, Rev. Mod. Phys. **83**, 1057 (2011).
[7] Z. Wang, H. Weng, Q. Wu, X. Dai, and Z. Fang, Phys. Rev. B **88**, 125427 (2013).
[8] Z. K. Liu, B. Zhou, Y. Zhang, Z. J. Wang, H. M. Weng, D. Prabhakaran, S.-K. Mo, Z. X. Shen, Z. Fang, X. Dai, Z. Hussain, and Y. L. Chen, Science **343**, 864 (2014).
[9] Z. Liu, J. Jiang, B. Zhou, Z. Wang, Y. Zhang, H. Weng, D. Prabhakaran, S.-K. Mo, H. Peng, P. Dudin, T. Kim, M. Hoesch, Z. Fang, X. Dai, Z. Shen, D. Feng, Z. Hussain, and Y. Chen, Nat. Mater. **13**, 677 (2014).
[10] M. Neupane, S.-Y. Xu, R. Sankar, N. Alidoust, G. Bian, C. Liu, I. Belopolski, T.-R. Chang, H.-T. Jeng, H. Lin, A. Bansil, F. Chou, and M. Zahid Hasan, Nat. Commun. **5**, 3786 (2014).
[11] X. Wan, A. M. Turner, A. Vishwanath, and S. Y. Savrasov, Phys. Rev. B **83**, 205101 (2011).
[12] A. A. Burkov, M. D. Hook, and L. Balents, Phys. Rev. B **84**, 235126 (2011).
[13] M. M. Vazifeh and M. Franz, Phys. Rev. Lett. **111**, 027201 (2013).
[14] H. Weng, C. Fang, Z. Fang, B. A. Bernevig, and X. Dai, Phys. Rev. X **5**, 011029 (2015).
[15] S.-M. Huang, S.-Y. Xu, I. Belopolski, C.-C. Lee, G. Chang, B. Wang, N. Alidoust, G. Bian, M. Neupane, C. Zhang, S. Jia, A. Bansil, H. Lin, and M. Z. Hasan, Nat. Commun. **6**, 7373 (2015).
[16] S.-Y. Xu, I. Belopolski, N. Alidoust, M. Neupane, G. Bian, C. Zhang, R. Sankar, G. Chang, Z. Yuan, C.-C. Lee, S.-M. Huang, H. Zheng, J. Ma, D. Sanchez, B. Wang, A. Bansil, F. Chou, P. Shibayev, H. Lin, S. Jia, and M. Hasan, Science **349**, 613 (2015).
[17] B. Q. Lv, H. M. Weng, B. B. Fu, X. P. Wang, H. Miao, J. Ma, P. Richard, X. C. Huang, L. X. Zhao, G. F. Chen, Z. Fang, X. Dai, T. Qian, and H. Ding, Phys. Rev. X **5**, 031013 (2015).
[18] S.-Y. Xu, N. Alidoust, I. Belopolski, Z. Yuan, G. Bian, T.-R. Chang, H. Zheng, V. Strocov, D. Sanchez, G. Chang, C. Zhang, D. Mou, Y. Wu, L. Huang, C.-C. Lee, S.-M. Huang, B. Wang, A. Bansil, H.-T. Jeng, T. Neupert, A. Kaminski, H. Lin, S. Jia, and M. Zahid Hasan, Nat. Phys. **11**, 748 (2015).
[19] C. Zhang, Z. Yuan, S. Xu, Z. Lin, B. Tong, M. Z. Hasan, J. Wang, C. Zhang, and S. Jia, arXiv:1502.00251.
[20] L. X. Yang, Z. K. Liu, Y. Sun, H. Peng, H. F. Yang, T. Zhang, B. Zhou, Y. Zhang, Y. F. Guo, M. Rahn, D. Prabhakaran, Z. Hussain, S.-K. Mo, C. Felser, B. Yan, and Y. L. Chen, Nat. Phys. **11**, 728 (2015).
[21] Z. Wang, Y. Zheng, Z. Shen, Y. Zhou, X. Yang, Y. Li, C. Feng, and Z.-A. Xu, arXiv:1506.00924.
[22] X. Huang, L. Zhao, Y. Long, P. Wang, D. Chen, Z. Yang, H. Liang, M. Xue, H. Weng, Z. Fang, X. Dai, and G. Chen, Phys. Rev. X **5**, 031023 (2015).
[23] B. Lv, N. Xu, H. Weng, J. Ma, P. Richard, X. Huang, L. Zhao, G. Chen, C. Matt, F. Bisti, V. Strocov, J. Mesot, Z. Fang, X. Dai, T. Qian, M. Shi, and H. Ding, Nat. Phys. **11**, 724 (2015).
[24] P. W. Anderson, Phys. Rev. **124**, 41 (1961).
[25] J. Kondo, Prog. Theor. Phys. **32**, 37 (1964).
[26] H. R. Krishna-murthy, J. W. Wilkins, and K. G. Wilson, Phys. Rev. B **21**, 1003 (1980).
[27] A. Tsvelick and P. Wiegmann, Z. Phys. B **54**, 201 (1984).
[28] N. Andrei and C. Destri, Phys. Rev. Lett. **52**, 364 (1984).
[29] F. C. Zhang and T. K. Lee, Phys. Rev. B **28**, 33 (1983).
[30] P. Coleman, Phys. Rev. B **29**, 3035 (1984).
[31] N. Read and D. Newns, J. Phys. C **16**, 3273 (1983).
[32] Y. Kuramoto, Z. Phys. B **53**, 37 (1983).
[33] O. Gunnarsson and K. Schönhammer, Phys. Rev. Lett. **50**, 604 (1983).
[34] I. Affleck, Nucl. Phys. B **336**, 517 (1990).
[35] H. Ishii, J. Low Temp. Phys. **32**, 457 (1978).
[36] V. Barzykin and I. Affleck, Phys. Rev. B **57**, 432 (1998).
[37] L. Borda, Phys. Rev. B **75**, 041307 (2007).
[38] C. Gonzalez-Buxton and K. Ingersent, Phys. Rev. B **57**, 14254 (1998).
[39] L. Fritz and M. Vojta, Phys. Rev. B **70**, 214427 (2004).
[40] M. Vojta and L. Fritz, Phys. Rev. B **70**, 094502 (2004).
[41] T. Shirakawa and S. Yunoki, Phys. Rev. B **90**, 195109 (2014).
[42] A. K. Mitchell and L. Fritz, Phys. Rev. B **92**, 121109 (2015).
[43] C. M. Varma and Y. Yafet, Phys. Rev. B **13**, 2950 (1976).
[44] V. Aji, C. M. Varma, and I. Vekhter, Phys. Rev. B **77**, 224426 (2008).
[45] X.-Y. Feng, W.-Q. Chen, J.-H. Gao, Q.-H. Wang, and F.-C. Zhang, Phys. Rev. B **81**, 235411 (2010).
[46] L. Fu and E. Berg, Phys. Rev. Lett. **105**, 097001 (2010).
[47] K. Sengupta and G. Baskaran, Phys. Rev. B **77**, 045417 (2008).
[48] H.-B. Zhuang, Q.-F. Sun, and X. Xie, Europhys. Lett. **86**, 58004 (2009).
[49] A. Principi, G. Vignale, and E. Rossi, Phys. Rev. B **92**, 041107 (2015).